

This article was downloaded by:

On: 23 January 2011

Access details: *Access Details: Free Access*

Publisher *Taylor & Francis*

Informa Ltd Registered in England and Wales Registered Number: 1072954 Registered office: Mortimer House, 37-41 Mortimer Street, London W1T 3JH, UK



Journal of Liquid Chromatography & Related Technologies

Publication details, including instructions for authors and subscription information:

<http://www.informaworld.com/smpp/title~content=t713597273>

Effect of β -Value on the Head and Tail Distribution of the Upper and Lower Phases in Helical Coils

Philip L. Wood^a; Barry Jaber^a; Lee Janaway^a; Nick Terlinden^a; Ian A. Sutherland^a

^a Brunel Institute for Bioengineering, Brunel University, Uxbridge, UK

To cite this Article Wood, Philip L. , Jaber, Barry , Janaway, Lee , Terlinden, Nick and Sutherland, Ian A.(2005) 'Effect of β -Value on the Head and Tail Distribution of the Upper and Lower Phases in Helical Coils', *Journal of Liquid Chromatography & Related Technologies*, 28: 12, 1819 – 1837

To link to this Article: DOI: 10.1081/JLC-200063466

URL: <http://dx.doi.org/10.1081/JLC-200063466>

PLEASE SCROLL DOWN FOR ARTICLE

Full terms and conditions of use: <http://www.informaworld.com/terms-and-conditions-of-access.pdf>

This article may be used for research, teaching and private study purposes. Any substantial or systematic reproduction, re-distribution, re-selling, loan or sub-licensing, systematic supply or distribution in any form to anyone is expressly forbidden.

The publisher does not give any warranty express or implied or make any representation that the contents will be complete or accurate or up to date. The accuracy of any instructions, formulae and drug doses should be independently verified with primary sources. The publisher shall not be liable for any loss, actions, claims, proceedings, demand or costs or damages whatsoever or howsoever caused arising directly or indirectly in connection with or arising out of the use of this material.

Effect of β -Value on the Head and Tail Distribution of the Upper and Lower Phases in Helical Coils

Philip L. Wood, Barry Jaber, Lee Janaway, Nick Terlinden,
and Ian A. Sutherland

Brunel Institute for Bioengineering, Brunel University, Uxbridge, UK

Abstract: To fully understand the motion of a point P mounted on a coil of a J-type centrifuge countercurrent chromatograph (CCC) requires the position, acceleration, and velocity to be known for any time t . The equations that determine the position and acceleration are well known, but the equation of the velocity is not. This paper derives the equations of velocity in the radial and tangential directions completing the description of the motion of the point P.

$$\text{Radial Velocity} = R\omega \sin(\omega t) \text{ and Tangential Velocity} = R\omega[\cos(\omega t) + 2\beta]$$

These equations show that the absolute velocity for a β -value of 0.5 is zero at the proximal key node. This β -value may act as an important division in the hydrodynamics of CCC as the β -value of 0.25 does. To date, the study of the hydrodynamics of CCC has been divided into two regions: that with β -values between 0 and 0.25 and everything above a β -value of 0.25. This new division may create a third region of hydrodynamic behaviour. The three β -value regions being: 0 and 0.25, between 0.25 and 0.5 and, finally, above 0.5. This paper provides experimental results showing how the head-tail relationship for hydrophobic, intermediate, and hydrophilic phase systems change at a β -value of 0.5 with a possible explanation.

Keywords: Please supply

INTRODUCTION

It has published results from an investigation into the effect of β -value on the retention and head and tail preferences of the upper and lower phase for a large

Address correspondence to Philip L. Wood, Brunel Institute for Bioengineering, Brunel University, Uxbridge, UB8 3PH, UK. E-mail: philip.wood@brunel.ac.uk

number of phase systems. The head end of a helical coil, orientated with its main axis horizontal, is the end that a bubble or bead would move towards when the coil was rotated about its main axis. The tail is the opposite end of the coil. The head and tail ends of a coil switch when the direction of rotation is changed.

This investigation covered both helical and spiral coils. In part of this study he used three helical coils on three different radii bobbins. The radii of these bobbins were 25 mm, 50 mm, and 75 mm. Phase distribution studies were conducted on these bobbins using two different rotor radii; these radii were 100 mm and 200 mm. This means that each helical coil was tested at two β -values. At a rotor radius of 100 mm these values were 0.25, 0.5, and 0.75, and at a 200 mm rotor radius the β -values were 0.125, 0.25, and 0.375, respectively. Each helical coil was wound from 1.6 mm bore tubing that had a 2.4 mm outside diameter; this means that the helical pitch of each coil was 2.4 mm. This helical pitch, combined with a coil (bobbin) radius, allows the helix angle to be calculated for each coil; the helix angles are 0.875° (25 mm), 0.438° (50 mm), and 0.292° (75 mm). This means the helix angle of the 75 mm coil is approximately a third of the 25 mm coil and the helix angle of the 50 mm coil is approximately half that of the 25 mm coil. This comparison of helix angles shows that another variable has possibly been inadvertently introduced into this study, which may affect the retention of stationary phase in an unknown way; hence, these results cannot be attributed to β -value alone. Also, the results presented in Figures 2A and 3A from Ref.^[1] are confusing given that the horizontal axes have different rotational speed ranges. Figure 2A shows phase distribution diagrams for the $R = 200$ mm centrifuge, which has a speed range from 200 to 800 rpm. Figure 3A shows similar phase distribution diagrams for the $R = 100$ mm centrifuge over a speed range from 400 to 1000 rpm. It is easier to compare these figures over the 400 to 800 rpm range only. Ito found that the stationary phase retention improved for most phase systems above a β -value of 0.5, and that the hydrodynamic behaviour inverted for some phase systems at this β -value.

Ito^[1] also compared stationary phase retention results for two spiral coils wound from 1.6 mm bore tubing (2.4 mm external diameter) and 2.6 mm bore tubing (3.6 mm external diameter) rotated on a 100 mm rotor radius, both with β -value value ranges from 0.5 to 0.8. To try and maintain similar flow velocities, Ito doubled the flow rates in the 2.6 mm bore coil compared with the 1.6 mm bore coil. To obtain similar flow velocities the flow rates should have been increased by the ratio of the cross-sectional areas, i.e., approximately 2.64. Therefore, the mobile phase flow rate for the hexane, ethyl acetate, and chloroform phase systems should have been 5.3 mL/min and not 4 mL/min as used. Also, for the butanol phase systems, the flow rate should have been approximately 2.6 mL/min and not 2 mL/min as used. To truly compare the effect of changing the bore size on retention, the same flow rates should have been used in both spiral coils. The spiral pitch, a

factor of the external diameter of the tubing, of both coils should also have remained a constant, i.e., 3.6 mm. Therefore, the results presented in this paper must be interpreted bearing these factors in mind. Examination of Figure 4A from Ref.^[1] shows that the % of stationary phase retention for the hydrophobic (hexane-water, ethyl acetate-water, and chloroform-water) phase systems are higher at rotational speeds between 400 and 600 rpm, and are of similar values above 600 rpm for the 2.6 mm bore coils. Similar statements can also be made for the intermediate (hexane-methanol, ethyl acetate-acetic acid-water (4:1:4), chloroform-acetic acid-water (2:2:1), and n-butanol-water) phases systems. Mindful that the flow rates were doubled for the 2.6 mm bore coil indicates the ability of this coil to retain stationary phase at higher flow rates, is greater than the 1.6 mm bore coil.

The results for the hydrophilic (n-butanol-acetic acid-water (4:1:5) and sec.-butanol-water) phase systems in the 1.6 mm bore coil are interesting in that the head and tail preferences of the upper and lower phases are different than the other phase systems. For the hydrophobic and intermediate phase systems the upper phase has a preference for the head end of the coil and the lower phase has a preference for the tail end. The best retention is obtained when the coil is operated with the head at the centre and the tail at the periphery. However, for the hydrophilic phase systems the head and tail preferences are reversed, with the upper phase going to the tail and the lower phase to the head. However, the best retention of stationary phase is still obtained when the coil is operated with the head at the centre and the tail at the periphery. The head and tail preferences of the hydrophilic phase systems in the 2.6 mm bore coil switch at 700 rpm for one result and at 900 rpm for the other three results, which are indicated by the thick solid lines and the thick dashed lines crossing each other. This means that if larger bore coils are rotated quickly enough all phase systems have the same head and tail preferences, meaning that the same operating conditions for the best stationary phase retention are identical for all phase systems, i.e., those described above for hydrophobic and intermediate phase systems.

Sutherland et al.^[2] also investigated retention in a spiral coil using a 100 mm rotor radius but with coils wound from transparent 3.18 mm bore FEP (Fluorinated Ethylene Propylene) tubing that had an external diameter of 4.76 mm. This coil had a β -value range of 0.38 to 0.85 and was rotated at 800 rpm. The original aim of this study was to significantly reduce the effects of viscosity on the results by using the larger bore tubing. A number of the same phase systems as those used by Ito^[1] were tested in this coil, along with other hydrophobic, intermediate, and hydrophilic phase systems. Each phase system was tested with the coil orientated tail-centre head-periphery and head-centre, tail-periphery. Ito^[1] measured the stationary phase retention in both coil orientations with both the lower and upper phases as the mobile phase, whereas Sutherland et al.^[2] performed head and tail studies. In a head and tail study transparent coils are used, the upper and

lower phases are dyed different colours. The coil is completely filled with equal proportions of dyed upper and lower phase, and then each end of the coil is sealed. The distribution of the upper and lower phases is recorded after which the coil is rotated in one direction for a given period. When rotation has stopped, the distribution of the upper and lower phases is again recorded. Comparison of the phase distribution from before and after rotation indicates which phase is driven towards the head and which phase towards the tail. The test can then be repeated rotating the coil in the other direction to change the orientation of the coil to determine this orientation's effect upon the phase distribution.

When the coil was orientated tail-centre head-periphery the lower phase did not always collect at the tail and upper phase at the head. Which phase collected at each end of the coil depended upon whether the phase system tested was hydrophobic, intermediate, or hydrophilic. These results were very similar to those found by Ito.^[1]

The research showed the lower phase always accumulated at the tail and the upper phase at the head, when a spiral coil was orientated head-centre tail-periphery. In this coil configuration the Archimedean screw effect and the hydrostatic pressure, generated in a spiral coil, combine to produce the same behaviour for each phase system regardless of whether the phase system was hydrophobic, intermediate, or hydrophilic. This confirmed that in larger bore tubing, where the viscous effects of the tubing wall are significantly reduced, all phase systems exhibit the same general hydrodynamic behaviour. The main recommendation of Sutherland et al.^[2] was to always rotate the coil in a direction that orientates the coil head-centre tail-periphery to provide the best stationary phase retention. However, the affects of β -value were not fully investigated, but the following statements were made. The clockwise rotation orientated the coil head-centre tail-periphery. Examination of Figure 5A of Ref.^[2] for the heptane/water (1:1 v:v) phase system (a hydrophobic phase system) shows the tail completely occupied by the lower phase and that the upper phase completely fills the heads. However in Figures 5C and 5E from Ref.^[2] the head is not completely filled with upper phase. Figure 5C represents a result for the same conditions as shown in Figure 5A for the ethyl acetate/acetic acid/water (4:1:4, v:v:v), an intermediate phase system. For Figure 5C, Sutherland et al. stated "it can be seen that for clockwise rotation the heavy phase moves to the tail, but below a β -value of 0.55 movement is much more sluggish". Figure 5E represents a similar result, to Figure 5C, for the n-butyl alcohol/acetic acid/water (4:1:5, v:v:v), a hydrophilic phase system. For Figure 5E, Sutherland et al. also stated "it can be seen that for clockwise rotation the heavy phase still moves to the tail, and again, below a β -value of 0.55, there are remnants of the lower phase lingering at the "head". From these statements it can be seen that there is something significant occurring at a β -value of 0.55, or close to this value. Figures 6C, 6E, and 6G from Ref.^[2] also show similar results to Figures 5C and 5E.

Theory

To fully describe and understand the motion of a point in space, its position, velocity, and acceleration change with respect to time must be known. Conway^[3] plots the position and gives equations for the radial and tangential accelerations of a point P on a coil throughout one revolution of a J-type centrifuge for various β -values. The equation for radial acceleration shows that for a β -value of 0.25 the radial acceleration is zero at the proximal key node. Below a β -value of 0.25 the radial acceleration switches from pointing inwards to outwards close to the proximal key node, causing a mixing process similar to cascade mixing^[4] when applied to a two-phase liquid system. (The proximal key node is when the point P is closest to the main axis of a J-type centrifuge. This main axis is represented in Figures 1 and 2 by the origin. In Figure 3, the 180° position on the horizontal axis represents the proximal key node.) For β -values above 0.25 the radial acceleration always points inwards allowing density stratification of the upper and lower phases to occur, resulting in wave mixing.^[4] The following derives the equation for radial and tangential velocity of the point P, and shows that the point P is stationary at the proximal key node for a β -value of 0.5.

From Figure 1, for the displacement of the point P in the x-direction, taking the centre of rotation as the origin, then differentiating to obtain formulas for velocity in the x-direction, remembering that $\theta = \omega t$ we obtain:

$$\text{Displacement x-direction: } x = R \cos(\omega t) + r \cos(2\omega t) \tag{1}$$

$$\text{Velocity x-direction: } \frac{dx}{dt} = -R\omega \sin(\omega t) - 2r\omega \sin(2\omega t) \tag{2}$$

$$\begin{aligned} \text{Now } \beta = \frac{r}{R} \quad \frac{dx}{dt} &= -R\omega \sin(\omega t) - 2\beta R\omega \sin(2\omega t) \\ \frac{dx}{dt} &= -R\omega(\sin(\omega t) + 2\beta \sin(2\omega t)) \end{aligned} \tag{3}$$

From Figure 1 resolving for the displacement of the point P in the y-direction taking the centre of rotation as the origin and then differentiating to obtain formulas for velocity in the y-direction we obtain:

$$\text{Displacement y-direction: } y = R \sin(\omega t) + r \sin(2\omega t) \tag{4}$$

$$\text{Velocity y-direction: } \frac{dy}{dt} = R\omega \cos(\omega t) + 2r\omega \cos(2\omega t) \tag{5}$$

$$\begin{aligned} \text{Now } \beta = \frac{r}{R} \quad \frac{dy}{dt} &= R\omega \cos(\omega t) + 2\beta R\omega \cos(2\omega t) \\ \frac{dy}{dt} &= R\omega(\cos(\omega t) + 2\beta \cos(2\omega t)) \end{aligned} \tag{6}$$

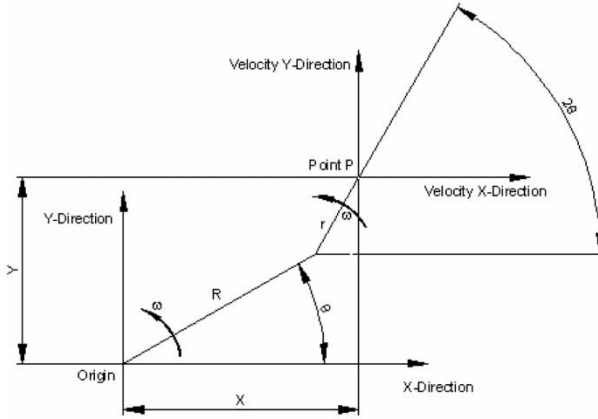


Figure 1. The free-body diagram for a J-type centrifuge.

These equations represent the motion of the point P in space relative to the origin, which is the main rotary axis of a J-type centrifuge. From Figure 2 resolving in the Radial and Tangential directions we obtain:

$$\text{Radial Velocity} = \frac{dx}{dt} \cos(2\omega t) + \frac{dy}{dt} \sin(2\omega t) \tag{7}$$

$$\text{Tangential Velocity} = -\frac{dx}{dt} \sin(2\omega t) + \frac{dy}{dt} \cos(2\omega t) \tag{8}$$

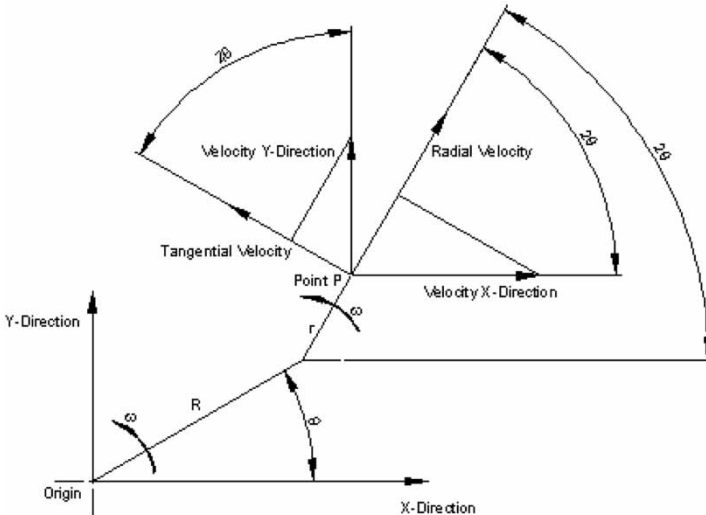


Figure 2. The free-body diagram of a J-type centrifuge with the radial and tangential velocity vectors added.

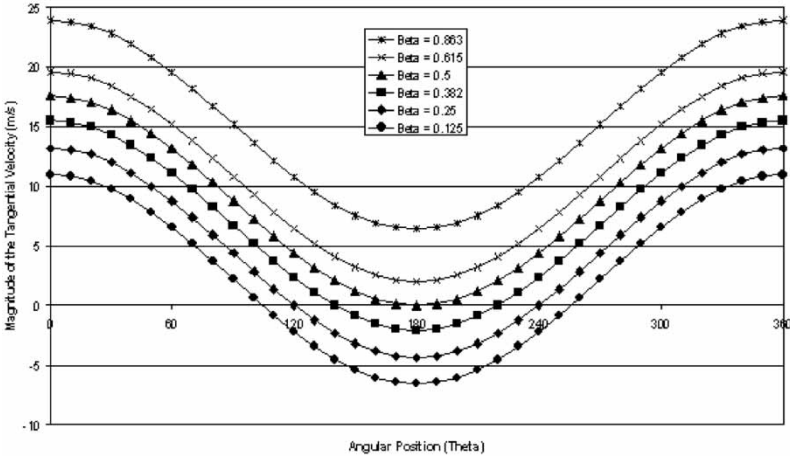


Figure 3. Tangential velocity versus angle for different β -values.

Substituting in Equation 7 for dx/dt from Equation 3 and for dy/dt from Equation 6 gives:

$$\begin{aligned}
 \text{Radial Velocity} &= -R\omega \cos(2\omega t)(\sin(\omega t) + 2\beta \sin(2\omega t)) \\
 &\quad + R\omega \sin(2\omega t)(\cos(\omega t) + 2\beta \cos(2\omega t)) \\
 &= -R\omega [\cos(2\omega t)(\sin(\omega t) + 2\beta \sin(2\omega t)) \\
 &\quad - \sin(2\omega t)(\cos(\omega t) + 2\beta \cos(2\omega t))] \\
 &= -R\omega [\cos(2\omega t) \sin(\omega t) + 2\beta \cos(2\omega t) \sin(2\omega t) \\
 &\quad - \sin(2\omega t) \cos(\omega t) - 2\beta \sin(2\omega t) \cos(2\omega t)]
 \end{aligned}$$

$$\text{Radial Velocity} = -R\omega [\cos(2\omega t) \sin(\omega t) - \sin(2\omega t) \cos(\omega t)]$$

$$\text{Radial Velocity} = R\omega [\sin(2\omega t) \cos(\omega t) - \cos(2\omega t) \sin(\omega t)]$$

Using $\sin(A - B) = \sin(A) \cos(B) - \cos(A) \sin(B)$ where

$$A = 2\omega t \text{ and } B = \omega t$$

(9)

Therefore Radial Velocity = $R\omega \sin(\omega t)$

Since there is a no negative sign at the front of Equation 9, the direction of the Radial Velocity is in the same direction as that shown in Figure 2. Equation 9 also shows that the radial velocity will be zero whenever $\sin(\omega t)$ equals zero, which is when $\omega t = 0$ and 180° , i.e., the proximal and distal key nodes. (The distal key node is the position when the point P is furthest away from the main axis of the centrifuge or the origin in Figures 1 and 2. In Figure 3, the 0° and 360° positions along the horizontal axis represent the distal key node.). This equation also shows that the radial velocity does not change with β -value.

Substituting in Equation 8 for dx/dt from Equation 3 and for dy/dt from Equation 6 gives:

$$\begin{aligned}
 \text{Tangential Velocity} &= -\frac{dx}{dt} \sin(2\omega t) + \frac{dy}{dt} \cos(2\omega t) & (8) \\
 &= R\omega \sin(2\omega t)(\sin(\omega t) + 2\beta \sin(2\omega t)) \\
 &\quad + R\omega \cos(2\omega t)(\cos(\omega t) + 2\beta \cos(2\omega t)) \\
 &= R\omega[\sin(2\omega t)(\sin(\omega t) + 2\beta \sin(2\omega t)) \\
 &\quad + \cos(2\omega t)(\cos(\omega t) + 2\beta \cos(2\omega t))] \\
 &= R\omega[\sin(2\omega t) \sin(\omega t) + 2\beta \sin^2(2\omega t) \\
 &\quad + \cos(2\omega t) \cos(\omega t) + 2\beta \cos^2(2\omega t)]
 \end{aligned}$$

But $\cos^2(2\omega t) + \sin^2(2\omega t) = 1$ therefore:

$$\begin{aligned}
 \text{Tangential Velocity} &= R\omega[\sin(2\omega t) \sin(\omega t) \\
 &\quad + \cos(2\omega t) \cos(\omega t) + 2\beta] \\
 \text{Using } \cos(A - B) &= \cos(A) \cos(B) + \sin(A) \sin(B) \text{ where} \\
 A = 2\omega t \text{ and } B &= \omega t \\
 \text{Therefore } \cos(\omega t) &= \cos(2\omega t) \cos(\omega t) + \sin(2\omega t) \sin(\omega t) & (10)
 \end{aligned}$$

Therefore Tangential Velocity = $R\omega[\cos(\omega t) + 2\beta]$

Since there is no negative sign, the direction of the tangential velocity is anti-clockwise as shown in Figure 2. Equation 10 also shows that the tangential velocity will be zero when $[\cos(\omega t) + 2\beta] = 0$ and β has a positive, which is when $\cos(\omega t) = -1$ given these conditions $\beta = 0.5$. $\cos(\omega t) = -1$ when $\theta = 180^\circ$, which is the proximal key node. (β -values can only be positive since β -values are the ratio of the coil radius to the planetary radius and to be negative would require a negative radius.). Therefore, at the proximal key node for a β -value of 0.5 the tangential velocity of the point P is zero. Also, at the proximal key node for all β -values the radial velocity of the point P is also zero, see above. Therefore, the total velocity of the point P at the proximal key node for a β -value of 0.5 is zero, i.e., the point P is stationary. However any liquids adjacent to the point P will continue to move due to their momentum.

For β -values below 0.5, the tangential velocity at the proximal key node is negative indicating a change in direction. For β -values above 0.5, this velocity is positive but has its lowest value at the proximal key node, see Figure 3. Figure 3 was generated for a rotor radius (R) of 100m and a rotational speed of 763 rpm. Equation 10 also shows that the tangential velocity is a maximum when $\cos(\omega t) = 1$ when $\theta = 0^\circ$, which is the distal key node for all β -values, this is also shown in Figure 3.

EXPERIMENTAL

The experimental method used to produce the following results is described in Chapter 2 section 2.8 of the Wood's Ph.D. thesis^[5] and is similar to that previously used,^[2] but adapted for helical coils used in a Brunel CCC J-type centrifuge.

A rotational speed of 763 rpm is used for the experimental studies conducted in this work, as this speed gives the same tangential acceleration at a rotor radius of 110 mm as 800 rpm gives at a rotor radius of 100 mm. This allows the results of these studies to be compared directly to previous ones.^[2]

The 4A, 4B and 4C phase systems, described below in Table 1, were studied in the FEP coils. These systems are classified as hydrophobic, intermediate, and hydrophilic, respectively.

Procion Brilliant Yellow dye was used to colour the lower aqueous phase of each solvent system. Similarly, Sudan Blue dye was used to colour the upper organic phase of each phase system. In the black and white reprints, Figures 4 to 12 shown in this paper, the upper organic phase appears black and the lower aqueous phase is clear.

The coils used were wound from similar lengths of tubing to maintain similar volumes, hence, the greater the β -value the lower the number of loops for each coil. The helical pitch was increased proportionally to the increase in β -value to keep the helix angle constant for each coil to keep another possible variable constant. The helix angle determines the orientation of the helically wound tubing containing the immiscible solvents, to the tangential accelerations affecting the motion of these liquids. Imagine a constant pitch helix wound from tubing around a cylinder, the tangential accelerations are aligned in plane perpendicular to the axis of the cylinder. The shallower the helix angle, the smaller the helical pitch, the closer the tubing will be aligned to the tangential accelerations.

The three FEP, (fluorinated ethylene propylene), coils were designed to have: three different β -values of 0.382, 0.615, and 0.863, for a rotor radius of 110 mm, and were selected to match the lowest, middle and highest β -values of the spiral coil previously used;^[2] approximately the same length of tubing (bore = 3.18 mm or 1/8 inch, outside diameter 4.76 mm or 3/16 inch) and approximately the same volume, 32.0 mL

Table 1. Showing the chemical composition of the phase systems and the ratios to which they are mixed

Phase system	Solvents	Ratios (by volume)
4A	Heptane–Ethyl acetate–Methanol–Water	1.4:0.1:0.5:1
4B	Heptane–Ethyl acetate–Methanol–Water	1.4:0.6:1 1
4C	Heptane–Ethyl acetate–Methanol–Water	1.4:4.5:1:1

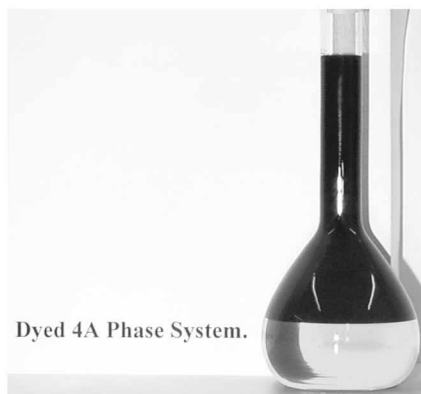


Figure 4. The upper organic phase was dyed in dark blue and the transparent lower phase of the 4A phase system was lightly yellow coloured.

(β -value = 0.382 coil), 34.3 mL (β -value = 0.615 coil) and 34.2 mL (β -value = 0.863 coil).

As β -value increases, the number of loops decreases, integer number of loops 16 (β -value = 0.382 coil), 10 (β -value = 0.615 coil) and 7 (β -value = 0.863 coil); the same helix angle, 1.09° , to maintain the same orientation of the tubing to the tangential acceleration.

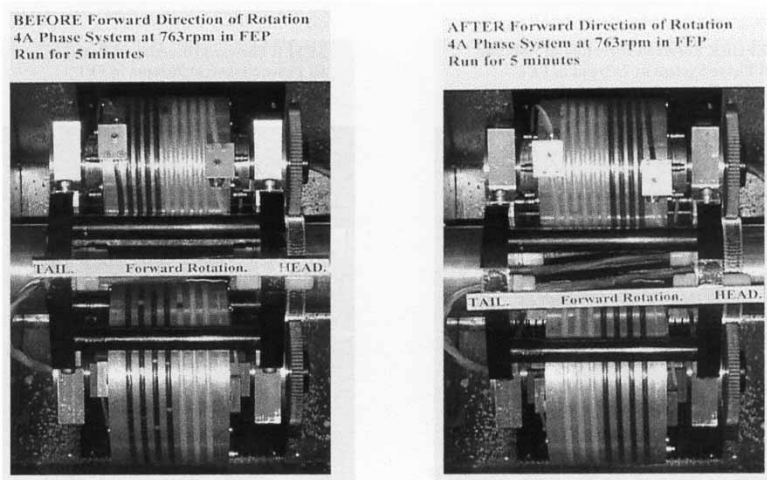


Figure 5. Head and tail distribution of the 4A phase system before and after 5 min rotation in the forward direction in both the 0.615 and 0.863 β -value coils. In the case of 5 min rotation in the reverse direction, the same picture was obtained but head was located on the left and tail on the right.

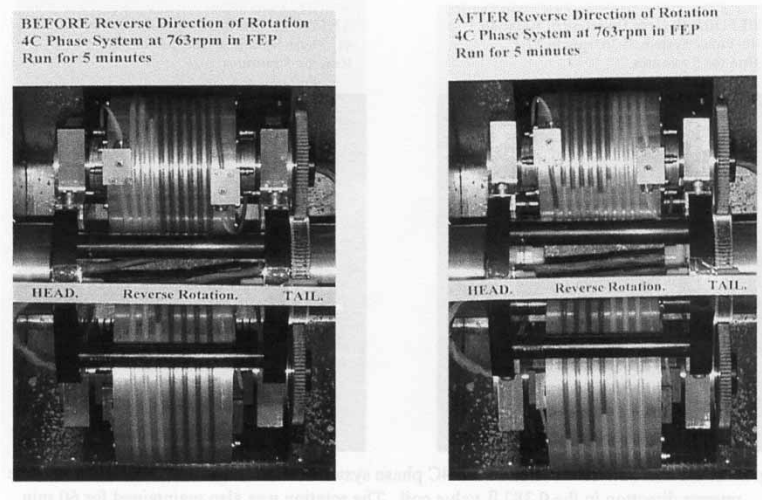


Figure 6. Head and Tail distribution of the 4C phase system before and after 5 min rotation in the reverse direction in both the 0.615 and 0.863 β -value coils. The rotation was also maintained for 60 min not showing any change.

The same helix angle at different β -values gives different helical pitches that increase with β -value. The helical pitches are 5.0 mm (β -value = 0.382 coil), 8.1 mm (β -value = 0.615 coil) and 11.3 mm (β -value = 0.863 coil).

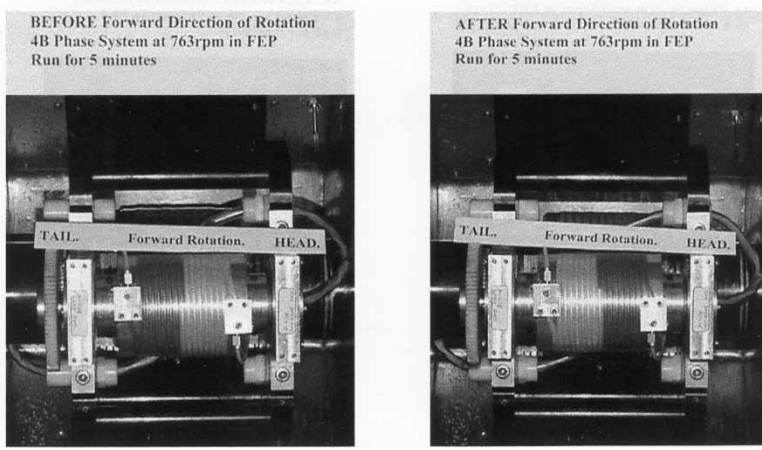


Figure 7. Head and tail distribution of the 4B phase system before and after 5 min rotation in the forward direction in the 0.382 β -value coil. In the case of 5 min rotation in the reverse direction, the same picture was obtained but head was located on the left and tail on the right.

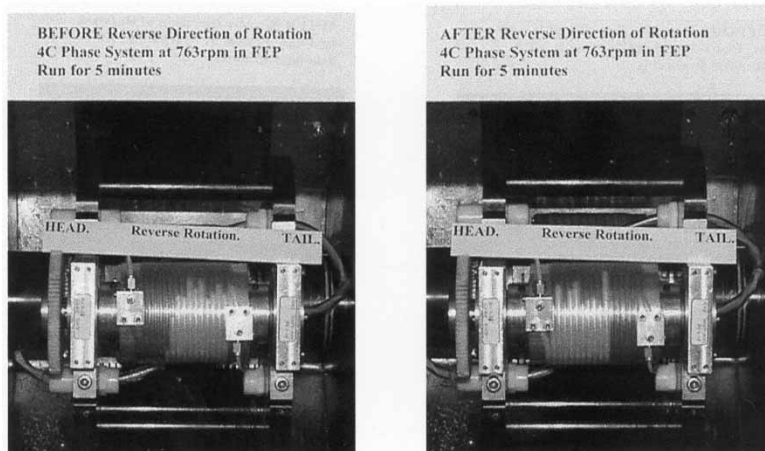


Figure 8. Head and tail distribution of the 4C phase system before and after 5 min rotation in the reverse direction in the 0.382 β -value coil. The rotation was also maintained for 60 min not showing any change.

RESULTS

Figure 4 shows that the upper organic phase for the 4A phase system was dyed blue, but appears black in Figures 4 to 12. This figure also shows that the lower aqueous phase was coloured yellow, but has a transparent or clear appearance in Figures 4 to 12. Identical pictures can also be shown for the 4B and 4C phase systems, but are not shown.

Head and Tail Studies in the 0.863 and 0.615 β -Value Coils

In Figs. 5 to 8, the 0.863 β -value coil is at the bottom and the 0.615 β -value coil is at the top of each photograph.

In Figs. 5 to 12 the forward direction of rotation is clockwise and the reverse direction is anti-clockwise, when viewed from the right hand side. Figures 5 and 9 show results for the forward direction of rotation, placing the tail of all three coils on the left hand side and the head on the right hand side. For the reverse direction of rotation, the head, for all three coils, is on the left hand side and the tail is on the right hand side, in Figs. 6, 7, 8, 10, 11, and 12.

Figures 5 and 6 show that the black upper phase of the 4A phase distributes to the head end of both helical coils for both the forward and reverse directions of rotation. These figures also show that the clear lower phase of the 4A phase system distributes to the head end of both coils in both directions of rotation.

Identical results to those shown in Figures 5 and 6 were obtained for the 4B phase system. These results are not shown to reduce duplication of similar figures.

Figures 7 and 8 display the results for the 4C phase system in the 0.863 and 0.615 β -value coils. The right hand photograph of Figure 7 shows the distribution of darker upper phase at the head and the lower transparent phase at the tail end of both coils after 5 minutes of rotation in the reverse direction. Although the tail end of both coils are completely filled with lower phase there is still some lower at the head end of each coil. Again identical results were obtained for the forward direction of rotation after 5 minutes.

Figure 8 shows the distribution after a total of 60 minutes of rotation in the reverse direction, the distribution had not altered that from that obtained after 5 minutes see Figure 7. (The times shown on the photographs are the total time rotating in the appropriate direction. Therefore, the photograph taken after 60 minutes was taken after 55 more minutes of rotation after the right hand photograph in Figure 7.

Head and Tail Studies in the 0.382 β -Value Coil

Figures 9 and 10 show, for the 4B phase system, the upper darker phase distributes to the head end of a coil regardless of the direction of rotation. The lower transparent phase distributes to the tail end of a coil also regardless of the direction of rotation. Identical results were also obtained for the 4A phase system.

For the 4C system, Figure 11 shows that the tail is completely occupied by the darker upper phase while the head end of the coil contains a mixture of both phases. The same head and tail distribution is shown after a total of 60 minutes of rotation in Figure 12. The starting positions of the upper and lower phases in Figure 11 for the 4C system are different to those for the 4B phase system shown in Figure 10. The first test of the 4C system in the 0.382 β -value coil had the same starting position as the 4B system however the 4C system did not move after rotation. It was only after switching the starting positions of the upper and lower phases that rotation in the reverse direction causes the upper and lower phases to change ends.

DISCUSSION

Head and Tail Studies in the 0.863 and 0.615 β -Value Coils

The head and tail results show that, for coils with β -values above 0.5, the less dense upper phase always distributes to the head end of the coil regardless of the direction of rotation. Similarly, the denser lower phase always distributes to the tail end of the coil and again is not influenced by the direction of rotation. For the hydrophobic (4A) and intermediate (4B) phase systems the

head and tail ends are completely filled with a single phase. For the hydrophilic (4C) phase system the tail ends of both coils were completely filled with the lower phase. However, the head ends of these coils were not completely filled with the upper phase see of the 4C phase system, see Figures 7 and 8, there are small amounts of lower phase present.

Head and Tail Studies in the 0.382 β -Value Coil

The same head and tail distribution for the hydrophobic (4A) and intermediate (4B) phase systems in the 0.382 β -value coil was obtained as in both the 0.615 and 0.863 coils. However, the distribution of the hydrophilic (4C) phase system in the 0.382 β -value coil is different to these other coils. The 4C upper phase completely fills the tail end; however, the head end is filled with both upper and lower phases. In the 0.615 and 0.863 β -value coils, the 4C lower phase completely filled the tail end and the head end contained a mixture. It is interesting to note that the head end of each coil contained both phases of the hydrophilic (4C) phase system while the tail ends were completely filled with a single phase. The tail ends of the 0.615 and 0.863 β -value coils were filled with lower phase while the tail end of the 0.382 coil was filled with upper phase. This demonstrates a change in the head and tail distribution for the hydrophilic (4C) phase system when the 0.5 β -value is crossed.

Archimedean Screw Action

Archimedean action tries to screw both phases towards the head end of a coil. Usually, one phase occupies the head while the other fills the tail. For the 4A and 4B phase systems the upper phase completely fills the head while the lower phase occupies the whole of the tail.

Table 2 shows the physical properties of the three phase systems used. Interfacial tension does not directly affect the head and tail distribution in these three coils as each coil was wound from 3.18 mm internal diameter tubing, which cannot be classified as a capillary bore. The dynamic viscosity of both the upper and lower phases from each solvent system are approximately the same, hence viscosity cannot be driving the distribution of the upper and lower phases in these coils. The density difference of the 4C phase system is less than half that of the other two-phase systems hence density difference must be driving the observed distribution shown in Figs. 5 to 12. It is worth emphasizing that the J-type is a centrifuge and density difference is the basis of physically separating substances in centrifuges. In a simple, single axis, laboratory centrifuge the acceleration is directed towards the centre of rotation, however the pressure in a liquid increases radially outwards from the centre of the coil. If the upper and lower phases were present in a radially aligned test tube, the lower phase would collect at

Table 2. Showing the physical properties of the phase systems, at 30°C

Phase system	Density (kg/m ³)	Density diff. (kg/m ³)	Dynamic viscosity cp (mNs/m ²)	Interfacial tension (mN/m)
4A Upper	679	268	0.36	17.8
4A Lower	947		1.36	
4B Upper	708	230	0.35	6.2
4B Lower	938		1.35	
4C Upper	833	98	0.42	1.1
4C Lower	931		1.35	

This table was taken from Ref.^[6].

the radially outer most position displacing the upper phase towards the centre. Archimedean screw action accelerates both phases towards the head end of a coil, hence, in a similar way to the simple centrifuge the hydrostatic pressure increases towards the tail end of a coil. This means that the lower phase will collect at the tail end of a coil displacing the upper phase towards the head.

The 4A and 4B phase systems exhibit this behaviour in all three coils. However, if the density difference between the phases is low, as in the 4C system, the hydrostatic pressure difference between the phases maybe too small to produce an unambiguous head and tail distribution. This has been observed at the head end of all three coils for the 4C phase system.

To explain this more accurately requires a discussion regarding pressure gradients. In mechanically dynamic systems, such as centrifuges, pressure gradients are oriented in the opposite direction to the acceleration that creates the pressure gradient. A pressure gradient is the product (multiplication) of a fluid's density, the acceleration the fluid is experiencing and the distance from a reference point. The integration of a pressure gradient with respect to the reference point produces a hydrostatic pressure. This demonstrates that hydrostatic pressure is related to the fluid's position. The hydrostatic pressure produced depends upon the distance from a reference point and the density of the fluid. Two liquids with different densities at the same point (distance from a reference point) will have different pressures; the denser liquid will have the greater pressure. As stated earlier the Archimedean screw effect accelerates both phases towards the head, this makes it convenient for the reference point to be the head end of the coil, where the pressure is lowest. This means that the hydrostatic pressure will increase from the head towards the tail. As the upper and lower phases have different densities the rate at which the hydrostatic pressure increases for both phases will be different. The hydrostatic pressure in the lower phase will increase faster than that for the upper phase due to its greater density. This means that at the tail the lower phase will have the greater hydrostatic

pressure allowing it to displace the upper phase towards the head. In the case of the 4C phase system, with its low-density difference, the difference in hydrostatic pressures close to the head is too low to drive the phases to opposite ends of the coil. This means that both phases are present close to the head end of coils as observed in Figures 7, 8, 11 and 12.

Hydrodynamic Pressure

Archimedean screw action and its associated hydrostatic pressure does not explain why the upper phase of the 4C phase system collects at the tail end of a coil with a β -value less than 0.5, see Figures 11 and 12. To explain this requires the analysis of the tangential velocity and an understanding of hydrodynamic pressure.

Hydrodynamic pressure is the pressure that a fluid has due to its velocity, which is different to hydrostatic pressure where the pressure is related to the liquid's position. Bernoulli showed that for a fluid with no viscosity the total pressure was a constant related to its position and velocity. This means that as a fluid's position and velocity changed the total, or stagnation, pressure would remain the same; only the balance between the static and dynamic pressures would change. For a liquid solvent in a coil this means that the total pressure is related to its position and velocity. Equation 9 shows that the radial velocity of a point P on the tubing is a sine wave with amplitude $R\omega$ and is the same for all β -values. This means the radial component of hydrodynamic pressure is unaffected by β -value, however this is not the case for the tangential component of hydrodynamic pressure. Figure 3 plots the tangential velocity for various β -values. For β -values above 0.5 the tangential velocity is a cosine wave that does not have a negative portion. For β -values below 0.5 there is a negative portion of the cosine wave each side of the proximal key node. The lower the β -value the greater the portion that is negative. For example, the curve for a β -value of 0.382 shows that the velocity at the distal key node ($\theta = 0^\circ$ and 360°) is 15.5 m/s in the anticlockwise direction and is 2.1 m/s at the proximal key node ($\theta = 180^\circ$) in the clockwise direction. The change in direction from anticlockwise to clockwise occurs at roughly 140° and from clockwise back to anticlockwise at approximately 220° . This means that for about 40° of rotation before and after the proximal key node ($\theta = 180^\circ$) the point P is moving in the opposite direction compared to the majority of a revolution.

These changes of direction cause high shearing rates between the tubing wall and the phases. This shearing action may be high enough with low-density difference phase systems to generate a hydrodynamic pressure that is greater than the hydrostatic pressure causing the upper phase to be distributed to the tail end of coils with β -values less than 0.5. The hydrostatic pressure is still able to dominate when using high-density difference phase systems at β -values below 0.5. Above 0.5 there are no changes in the

direction of the tangential velocity. Hence shear rates and associated hydrodynamic pressures are not as great as those for coils below a β -value of 0.5 and the hydrostatic distribution dominates for all phase systems.

Mixing, Settling, and Turbulence

Traditionally, the mixing observed at the proximal key node has been attributed to Kelvin-Helmholtz instability of the interface.^[7] The tangential velocity of a point P on the tubing wall is the lowest at the proximal key node for β -values above 0.5. For values below 0.5 the direction of the tangential velocity changes direction close to the proximal key node. As the mobile and stationary phases are not fixed to the point P and are free to move relative to this point the tangential velocities experienced by these solvents will differ to that of the tubing. This relative movement between the solvents and the tubing wall will have a shearing effect leading to a velocity gradient dependent upon the distance from the tubing wall. Low velocity gradients indicate laminar flow while high velocity gradients show the presence of turbulence. Potentially high rotational speeds could cause steep velocity gradients and the associated shear turbulence in the solvents.

However, a change in direction of the tangential velocity, such as occurs below a β -values less than 0.5, should cause steeper velocity gradients and more turbulence than a simple slowing down of the tangential velocity, shown for coils with β -values greater than 0.5. Such differences in the amount of turbulence need to be taken into account when modelling the mixing and settling process. König^[8] has shown that computational fluid dynamics (CFD) can be used to model the mixing waves observed in CCC. The paper ends by stating that the future modelling work will include a single loop from a coil applying the associated radial and tangential accelerations to study wave motion and mass transfer between the solvents. Hopefully the work presented here will show the importance of the β -value and that two different β -value loops should be modelled, one in the range 0.25 to 0.5 and other above 0.5. In such modelling care should be taken to ensure that the radial and tangential velocities of the tubing and any accompanying shear turbulence are also taken into account.

Mass Transfer and Turbulence

To achieve high-resolution separations, high mass transfer rates are required. Turbulence is used to achieve high mass transfer rates. Simple calculations based upon the mobile phase flow rate and the stationary phase retention give low Reynolds numbers, indicating laminar flow^[9] and, hence, turbulence is not caused by the flow of the mobile phase. As discussed above turbulence is caused by the shearing action between the solvents and the tubing wall caused

by changes in the tangential velocity of the tubing. This shearing action combined with Kelvin-Helmholtz instability could explain the high mass transfer rates indicated by high-resolution chromatograms achieved using J-type centrifuges. Both these actions need to be considered when modelling: the mixing and settling processes; and the mass transfer rates indicated by high-resolution separations.

CONCLUSIONS

An explanation of the different hydrodynamic behaviour above and below a β -value of 0.5 has been given based upon an analysis of the tangential velocity of the point P on a coil.

Across the β -value range from 0 to 1 there are two critical values, which are 0.25 and 0.5. These values demarcate three distinct hydrodynamic processes. The first is between 0 and 0.25 and is similar to cascade mixing. The second is between 0.25 and 0.5 and the head and tail behaviour of a phase system depends upon whether it is a hydrophobic, intermediate or hydrophilic. The third range is from 0.5 to 1 where all phase systems exhibit the same head and tail preferences.

The retention theory that we presented by recently^[9] should only be used when modelling the retention behaviour of coils wound in the β -value range of 0.5 to 1. Caution should be used when applying this theory to coils wound in the 0.25 to 0.5 range.

Changes in the tangential velocity of the tubing could cause shear turbulence in the immiscible solvents within the tubing. The externally pumped flow of mobile phase flow does not cause this shear turbulence.

The modelling of the mixing and settling process inside a coil of a J-type centrifuge needs to take into account the radial and tangential velocities of the coil's motion and especially shear turbulence caused by changes in tangential velocity.

Shear turbulence caused by the changes in magnitude and direction of the tangential velocity should be considered when modelling the mass transfer rates in the coil of a J-type centrifuge.

REFERENCES

1. Ito, Y. Experimental observations of the Hydrodynamic behaviour of solvent systems in high-speed countercurrent chromatography, Part II. Phase distribution diagrams for Helical and spiral Columns. *J. Chromatogr.* **1984**, *301*, 387–403.
2. Sutherland, I.A.; Muytjens, J.; Prins, M.; Wood, P. A new hypothesis on the phase distribution in countercurrent chromatography. *J. Liq. Chromatogr. & Rel. Technol.* **2000**, *23* (15), 2259–2276.

3. Conway, W.D. *Countercurrent Chromatography Apparatus, Theory and Applications*; VCH Publishers: U.K., 1990.
4. Sutherland, I.A.; Heywood-Waddington, D.; Ito, Y. Counter-current chromatography, applications to the separation of biopolymers, organelles and cells using either aqueous-organic or aqueous-aqueous phase systems. *J. Chromatogr.* **1987**, *384*, 197–207.
5. Wood, P.L. The hydrodynamics of countercurrent chromatography in J-type centrifuges. Brunel University, 2002, Ph.D. Thesis.
6. Wood, P.L.; Jaber, B.; Sutherland, I.A. A new hypothesis on the hydrodynamic distribution of the upper and lower phase in CCC. *J. Liq. Chromatogr. & Rel. Technol.* **2001**, *24* (11&12), 1629–1654.
7. Sutherland, I.A.; Jones, S.; Heywood-Waddington, D.A. Preliminary study of the hydrodynamics of a range of solvent systems in a single layer coil planet centrifuge. *Preparative Countercurrent Chromatography*, No. 1045, Proc. Pittsburgh Conf., Atlantic City, N.J., March 1986.
8. König, C.S.; Sutherland, I.A. An investigation of the influence of the gravity field on the interface of two immiscible liquids—a computational study comparing prediction with experiment. *J. Liq. Chromatogr. & Rel. Technol.* **2003**, *26* (9&10), 1521–1535.
9. Wood, P.L.; Janaway, L.; Hawes, D.; Sutherland, I.A. Stationary phase retention in countercurrent chromatography: modelling the J-type centrifuge as a constant pressure drop pump. *J. Liq. Chromatogr. & Rel. Technol.* **2003**, *26* (9&10), 1373–1396.

Received October 18, 2004

Accepted November 29, 2004

Manuscript 6591CC